

MedChemComm

Accepted Manuscript



This is an *Accepted Manuscript*, which has been through the RSC Publishing peer review process and has been accepted for publication.

Accepted Manuscripts are published online shortly after acceptance, which is prior to technical editing, formatting and proof reading. This free service from RSC Publishing allows authors to make their results available to the community, in citable form, before publication of the edited article. This *Accepted Manuscript* will be replaced by the edited and formatted *Advance Article* as soon as this is available.

To cite this manuscript please use its permanent Digital Object Identifier (DOI®), which is identical for all formats of publication.

More information about *Accepted Manuscripts* can be found in the [Information for Authors](#).

Please note that technical editing may introduce minor changes to the text and/or graphics contained in the manuscript submitted by the author(s) which may alter content, and that the standard [Terms & Conditions](#) and the [ethical guidelines](#) that apply to the journal are still applicable. In no event shall the RSC be held responsible for any errors or omissions in these *Accepted Manuscript* manuscripts or any consequences arising from the use of any information contained in them.

Development of new *N*-Arylbenzamides as STAT3 Dimerization Inhibitors

Murali K. Urlam,^{†¶} Roberta Pireddu,^{†¶} Yiyu Ge,^{‡¶} Xiaolei Zhang,[†] Ying Sun,[†] Harshani R. Lawrence,^{†,‡,§} Wayne C. Guida,^{†,‡,¶} Saïd M. Sebtì,^{†,§,⊥} Nicholas J. Lawrence.^{†,§,*}

Departments of [†]Drug Discovery, and the [‡]Chemical Biology Core, Moffitt Cancer Center, 12902 Magnolia Drive, Tampa, FL 33612, USA

Departments of [§]Oncologic Sciences, [¶]Chemistry and [⊥]Molecular Medicine, University of South Florida, Tampa, FL 33620, USA

Corresponding Author: Nicholas J. Lawrence. E-mail: Nicholas.Lawrence@moffitt.org; Phone: +813 745 6037 (NJL), Fax: +813 745 6748

[¶] These authors contributed equally.

Abstract

The *O*-tosylsalicylamide **S3I-201** (**10**) was used as a starting point for design and synthesis of novel STAT-3 dimerization inhibitors with improved drug-like qualities. The phosphonic acid **12d** and salicylic acids **13f**, **13g** with a shorter amide linker lacking the *O*-tosyl group had improved STAT-3 inhibitory activity. The equivalent potencies observed by the replacement of phosphonic acid moiety of **12d** with 5-amino-2-hydroxybenzoic acid group as in **13f** further validates 5-amino-2-hydroxybenzoic acid as a phosphotyrosine mimic. The salicylic acid **13f** displayed improved whole cell activity. The focused library of salicylic acids **13** with benzamide linker indicated that hydrophobic heptyl and cyclohexyl are the best tolerated R groups and a biphenyl ether (as the Ar group) significantly contributes to STAT3 inhibitory activity. Our docking studies indicated that the acidic groups of **12d**, **13f** and **13g** interact in the p-Tyr-705 binding site in a broadly similar manner, while the phenoxybenzoyl group and the cyclohexylbenzyl group occupying pY+1 and pY-X hydrophobic pockets respectively. The *in vitro* and cell based potency of **13f** warrants further development of this scaffold as STAT3 inhibitors.

Introduction

STAT3 is a signal transducer and activator of transcription that transmits signals from cell surface receptors to the nucleus. STAT3 is frequently hyperactivated in many human cancers. Under normal conditions, STAT3 activation is transient and tightly regulated. Upon cellular stimulation by ligands such as growth factors or cytokines, STAT3 is phosphorylated on a critical tyrosine residue (Tyr705). This pTyr-STAT3 dimerizes through two reciprocal phosphotyrosine (pTyr)-Src-homology 2 (SH2) interactions. The STAT3 dimers then translocate to the nucleus and bind to specific DNA-response elements in the promoters of target genes thereby activating transcription.¹ STAT3 is found to be constitutively activated in many tumor cell types and contributes to tumor progression through the modulation of target of antiapoptotic genes such as Bcl-xL, Bcl-2, Mcl-1 and survivin along with genes driving cell cycle progression such as c-Myc and cyclin-D1.^{1, 2} The association of aberrant STAT3 activation with many types of human malignancies and solid tumors³ has made STAT3 an attractive molecular target for the development of novel cancer therapeutics.^{4, 5}

The design of compounds that target STAT3 has been the subject of several excellent reviews.^{6, 7} These include a survey of patents⁸ and a broader review of inhibitors of dimeric transcription factors.⁹ The direct targeting of STAT3 is a particularly attractive way to inhibit its function. Several approaches have been taken to inhibit the dimerization of phosphorylated STAT3 by blocking the SH2 domain binding site of the phosphorylated STAT3 tyrosine-705 residue. The first inhibitors of STAT3 dimerization were peptides and phosphopeptides.^{10, 11} Significant advances have been made by the groups of McMurray¹²⁻¹⁴ and Wang¹⁵ by using structure-based approaches resulting in potent peptide-like inhibitors incorporating a phosphotyrosine residue such as the pYLPQ mimics **1** and **2** respectively. These potent cell permeable STAT3 dimerization inhibitors have considerable ADME liabilities since the high affinity SH2 domain binding derives, at least in part, from the necessary presence of a hydrolyzable phosphate group or phosphonate prodrug. Indeed, to date, there are no reports of the activities of these compounds in animal models. As an alternative approach considerable attention has been paid to the discovery of non-peptidic small molecule drug-like inhibitors of STAT3 dimerization seeking to avoid some of the ADME challenges inherent in the development of peptide-

like inhibitors. Representative small molecule¹⁶ STAT3 dimerization inhibitors are shown in Figure 1 include the catechol **3**;¹⁷ the 1,3,4-oxadiazole **4**;¹⁸ the benzothiophene dioxide **5** (Stattic);¹⁹ the anthraquinone **6** (STA-21);²⁰ the purine **7**;²¹ the oxazole **8**;²² and the Celecoxib-like pyrazole **9**.²³

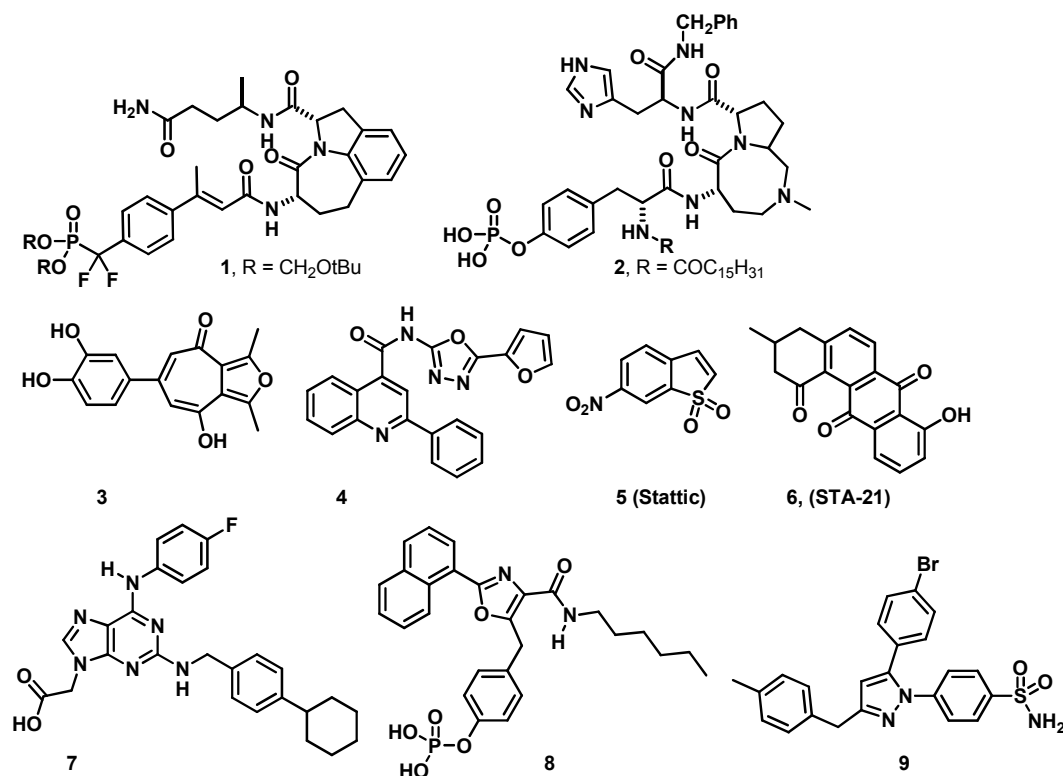


Figure 1. Chemical structures of representative STAT3 dimerization inhibitors

We identified the STAT3 inhibitor S3I-201 (**10**, NSC-74859)²⁴ (Figure 2) from the NCI chemical collection by using structure-based virtual screening with a model based on the X-ray crystal structure²⁵ of the STAT3 β homodimer (pdb code 1BG1). S3I-201 (**10**) inhibited STAT3:STAT3 complex formation and STAT3 DNA-binding and transcriptional activities. Furthermore, S3I-201 has been shown to exert antitumor effects against human breast²⁴ and liver²⁶ cancer xenografts in mouse models *via* mechanisms that are consistent with inhibition of STAT3 dimerization.

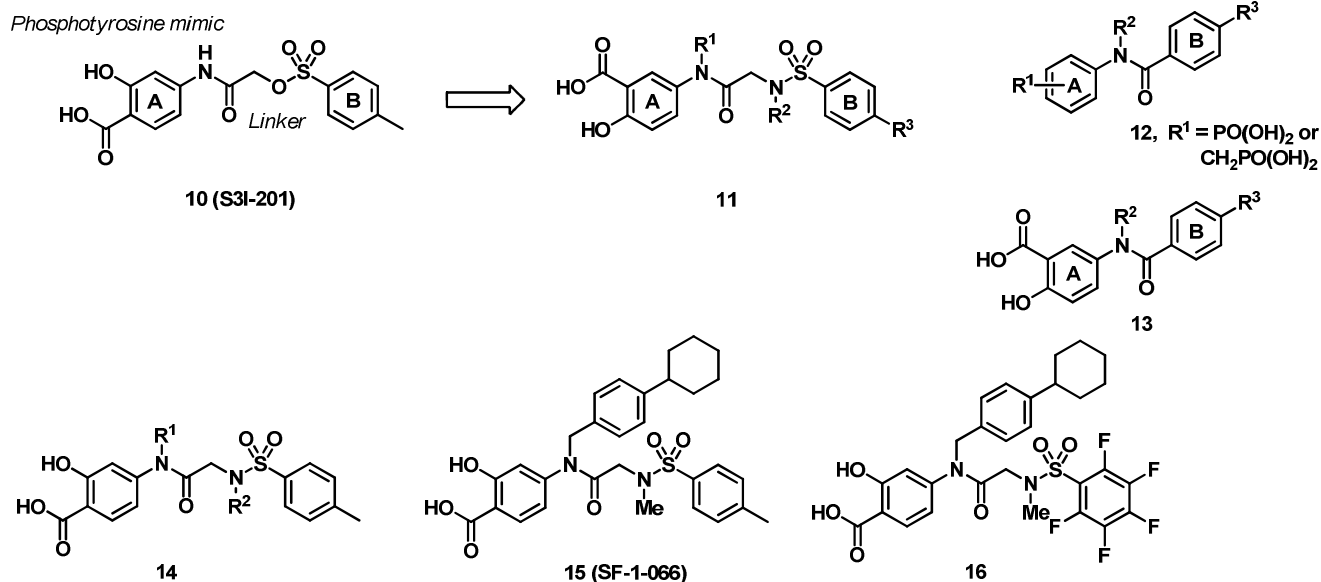


Figure 2. Chemical structures of S3I-201 (**10**, NSC-74859), scaffolds **12** and **13** and reported S3I-201 derivatives **14-16**.

In this communication, we describe our efforts toward improvement of S3I-201 (**10**). We focused on the replacement of the potentially reactive *O*-sulfonylglycine portion of **10**, and investigated alternative phosphotyrosine mimicking groups. We show that the phosphotyrosine mimicking 4-amino-2-hydroxybenzoic acid of **10** can be replaced by its isomeric partner 5-amino-2-hydroxybenzoic acid in the sulfonylglycine series **11**. We also show that the sulfonylglycine linker separating the two aryl groups of **11** by 5 atoms can be replaced by a shorter linker as in phosphonic acids **12** and salicylic acids **13**. Gunning and Turkson have developed a library **14**, based on **10**, in which the *O*-sulfonyl group has been replaced its *N*-sulfonyl counterpart.^{27, 28} The major findings of their work show that a large hydrophobic group as R¹ is beneficial, especially a *para*-cyclohexylbenzyl group. The analogs had an R² group as H, Me or BOC (*tert*-butyloxycarbonyl). The methyl containing compounds were the most potent. The sulfonamide **15** (SF-1-066) was shown to be the most potent in the fluorescence polarization assay (IC₅₀ 15-20 μM). Subsequently the pentafluorophenylsulfonamide **16** has been shown to be orally bioavailable and impressively inhibits the growth of human breast and lung tumor xenografts.²⁹

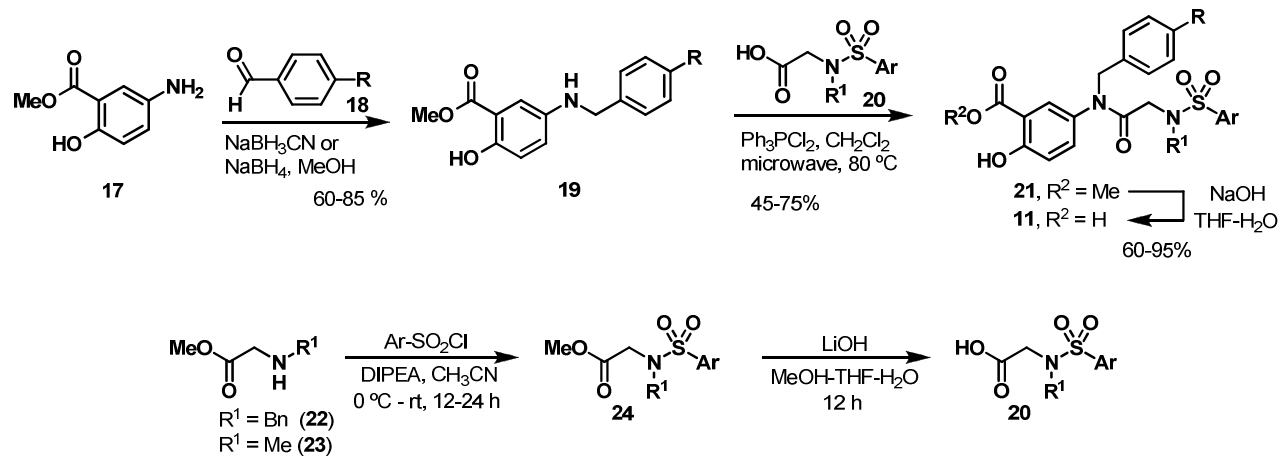
Results and Discussion

The routes to the analogs of **10** are shown in Schemes 1 and 2. First, the reductive amination of *para*-substituted arylaldehydes **18** with methyl 5-aminosalicylate (**17**) provided the corresponding *N*-arylmethylaminosalicylates **19** in good to excellent yields. The coupling reaction of the series of substituted aminosalicylates **19** with *N*-sulfonylglycine derivatives **20** was conveniently achieved following a modified procedure with dichlorotriphenylphosphorane (PPh_3Cl_2) to furnish the tertiary amides **21** in very good yields.³⁰ Subsequent hydrolysis of the methyl esters under basic conditions ($\text{NaOH-THF-H}_2\text{O}$) resulted in the formation of the desired salicylic acids **11**. The *N*-sulfonylglycine derivatives **20** were prepared from either *N*-benzyl or *N*-methyl glycine (**22** and **23** respectively) via *N*-sulfonylation with a range of substituted arylsulfonyl chlorides to first provide the sulfonamides **24** which were then hydrolyzed.

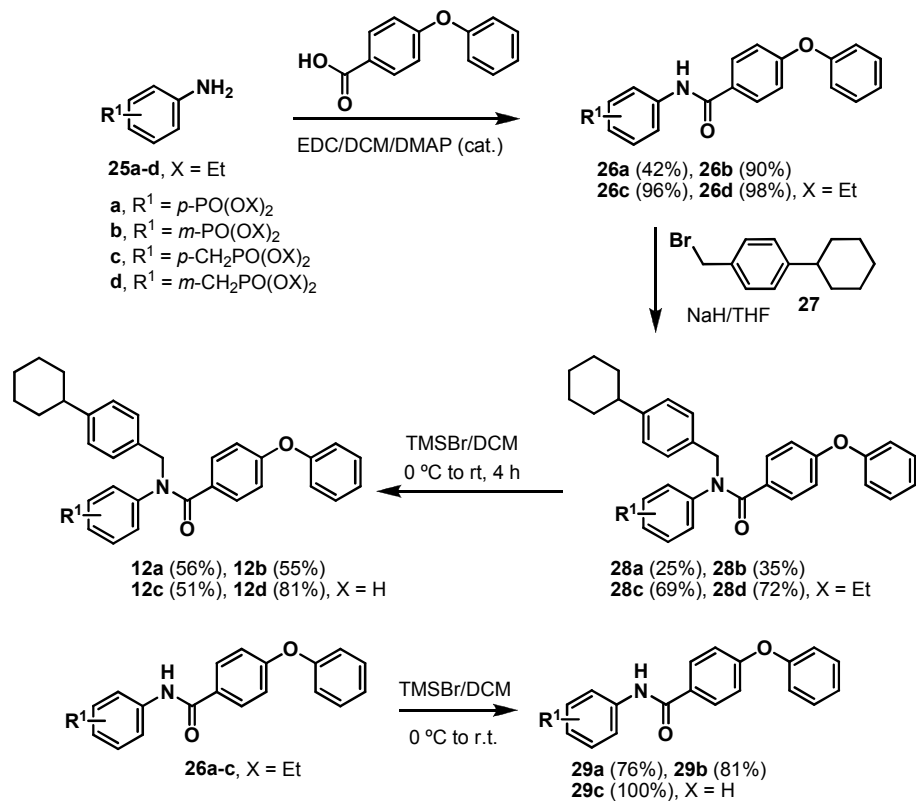
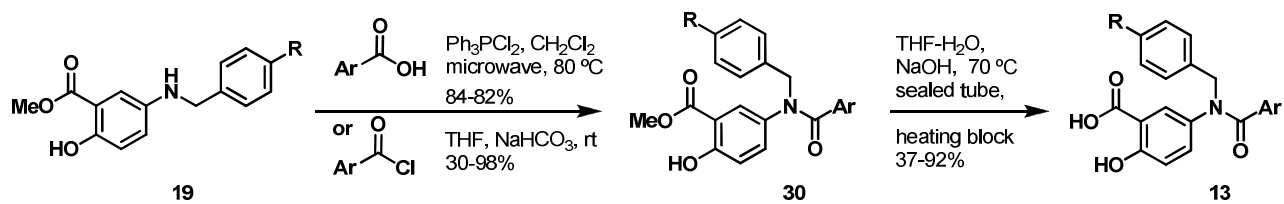
A library of related *N*-benzamides lacking the potentially reactive methylenoxysulfonyl group of **10**, incorporating an arylphosphonate (examples **12a** and **12b**) or benzylphosphonate (examples **12c** and **12d**) as a phosphotyrosine mimetic,³¹ was prepared as shown in Scheme 2. The amino diethyl phosphonate esters **25a,b,d** were prepared by methods shown in the supporting information (Scheme S1), whilst phosphonate **25c** was commercially available. The phosphonate-containing amides **26a-d** were prepared by coupling the amines **25a-d** with 4-phenoxybenzoic acid in the presence of EDC and catalytic amount of DMAP in DCM. This was followed by *N*-alkylation by treatment with sodium hydride and 1-(bromomethyl)-4-cyclohexylbenzene (**27**, see Scheme S1) in THF to provide the tertiary amides **28a-d**. The final phosphonic acids **12a-d** were obtained by treatment of **28a-d** with bromotrimethylsilane (TMSBr) (10 eq.) in dichloromethane. Similarly hydrolysis of the intermediate amides **26a-c** provided the phosphonic acid-containing amides **29a-c**. The library of *N*-benzamides **13** in which the phosphonic acid of **12** is replaced by a salicylic acid was prepared as shown in Scheme 3. The amide library **30**, incorporating a methyl salicylate, was prepared from the amine library **19**

(Scheme 1) *via* reaction with either a carboxylic acid and dichlorotriphenylphosphorane or directly with an acyl chloride. Finally, hydrolysis of the methyl salicylate ester of library **30**, performed in a sealed tube on a heating block, provided the desired library of salicylic acids **30** in good yields.

Scheme 1. Synthetic route to library 11



Scheme 2. Synthetic route to phosphonate containing benzamide analogs 12a-d

Scheme 3. Synthetic route to *N*-benzamide library 13

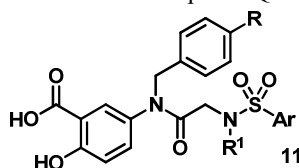
The ability of the libraries **11**, **12** and **13** to inhibit STAT3 dimerization was evaluated by a competitive, fluorescence-polarization (FP)-based assay, as developed by Schust and Berg,^{19, 32} and described in the Supporting Information, using full length STAT3 (N-terminal GST, SignalChem, Richmond, BC, Canada) and the fluorescent probe peptide 5-FAM-G(pTyr)LPQTV-CONH₂ (GenScript, Piscataway, NJ, USA).³² This peptide, derived from the gp130 IL6 receptor binds to the STAT3 SH2 domain; blocking its binding provides a measure of inhibition of STAT3 dimerization which binds through the sequence (pTyr)LKTKF.³³ Table 1 shows the STAT3 inhibitory activities of the library of sulfonamides **11** bearing a 5-amido-2-hydroxybenzoic acid group. Compound **11a**, which bears a tosyl group, equivalent to the sulfonyl B-ring of S3I-201, and a benzyl group on each nitrogen atom, is weakly active (**11a**, IC₅₀ = 201.3 ± 1.5 μM). When the tosyl group was replaced with a biphenylsulfonyl group, a 9-fold increase in the activity was observed (**11b**, IC₅₀ = 22 ± 9.1 μM) indicating that further analogs should be pursued. Although, the biphenylsulfonyl group appeared to be superior to the tosyl group, both series were prepared to further explore SAR relationship among these analogs. The *para*-chlorobenzyl derivative **11c** is 4-fold more potent (IC₅₀ = 50 ± 3.8 μM) than the unsubstituted analog **11a** (IC₅₀ = 201.3 ± 1.5 μM). Consistent with the above observations, the biphenylsulfonyl derivate (**11d**, IC₅₀ = 15 ± 1.2 μM) showed better activity than its tosyl analog **11c**. Other groups such methoxy, cyclohexyl, *n*-heptyl, and *iso*-butyl groups at the *para*-position of the amido *N*-benzylated derivatives (**11e**, **11f**, **11g** and **11h** respectively) resulted in activities similar to that of **11b** and **11d** (IC₅₀ values 17-23 μM).

The effect of a methyl group as the R¹ group was next assessed. Thus the library of *N*-methylsulfonamides **11i-r** was prepared as shown in Scheme 1 from commercially available sarcosine methyl ester (**23**). In most cases the *N*-methylsulfonamides, are less active than the corresponding *N*-benzylsulfonamide (R¹ = Bn) counterparts. For example the methyl group in the biphenylsulfonyl example **11j** (IC₅₀ = 57 ± 13 μM) and **11k** (IC₅₀ = 61 ± 6 μM), reduces activity compared to their respective benzyl analog **11b** (IC₅₀ = 22 ± 9.1 μM) and **11d** (IC₅₀ = 15 ± 1.2 μM). The presence of an alkyl benzyl group (R = cyclohexyl and *n*-heptyl, Table 1) in the *N*-methyl sulfonamides **11m** (IC₅₀ = 32 ± 12 μM) and **11n** (IC₅₀ = 22 ± 8 μM) did not alter their inhibitory as compared to the corresponding *N*-benzyl sulfonamides **11f** (IC₅₀ = 23.3 ± 2 μM) and **11g** (IC₅₀ = 19 ± 3.5 μM). Indeed the

presence of the cyclohexyl group dramatically improves the activity of the equivalent in tosylsulfonamide **11** ($IC_{50} = 45 \pm 12 \mu M$) (*cf.* unsubstituted benzyl derivative **11i**, $IC_{50} > 1000 \mu M$). This improvement was also seen with the 2-hydroxy-4-aminobenzoic acid series of Gunning and Turkson.²⁷ The tosylsulfonamide **11** ($IC_{50} = 45 \pm 12 \mu M$) is the isomeric form of **15** (**SF-1-066**) ($IC_{50} = 15 \pm 5 \mu M$, FP; $IC_{50} = 35 \pm 9 \mu M$, EMSA). In our hands the activity of **15** (**SF-1-066**) ($IC_{50} = 50 \pm 7.5 \mu M$, FP) is similar to that of **11**. We were unable to determine an IC_{50} of **11i** since it is so poorly active; the equivalent 2-hydroxy-4-aminobenzoic acid from Gunning and Turkson²⁷ (compound **14** in reference 27; $IC_{50} = 292 \pm 35 \mu M$, EMSA) is also significantly less active than its cyclohexyl substituted benzyl counterpart. Thus both isomers of the salicylic acid are of equivalent potency and improved over the IC_{50} of **10** (S3I-201) in the EMSA assay ($IC_{50} = 86 \pm 33 \mu M$, EMSA).^{27, 28} A chloro or fluoro biphenylsulfonamide group of the molecule (Ar) was tolerated (compounds **11o–11r**) showing similar activities to their biphenylsulfonamide where made. A small number of heterocyclic containing (as the R substituent) analogs **11s–11w** were prepared to reduce the overall lipophilicity of the compounds and provide a basic site for salt formation. The sulfonamides **11w** ($IC_{50} = 35.3 \pm 12.7 \mu M$) and **11t** ($IC_{50} = 33.5 \pm 1.8 \mu M$) possessing an *N*-benzylamide bearing a *meta*-4-pyridyl group had moderate inhibitory activity. The *N*-benzylamides **11s** ($IC_{50} > 300 \mu M$), **11u** ($IC_{50} = 94.7 \pm 0.32 \mu M$) and **11v** (14.4% inhibition at 50 μM) with heterocycles in the *para*-position were significantly less active.

We next focused on reducing the size of the glycine linker of **10** to separate the two aryl groups by 2 atoms by using a simple amide group as shown in **12** and **13** (Figure 1). We first made the *N*-benzamides **12a** and **12b** which incorporate an arylphosphonic acid as their non-hydrolyzable phosphotyrosine mimic, as shown in Scheme 2.³¹ The *para*-substituted isomer **12a** ($IC_{50} = 42.0 \pm 0.8 \mu M$) was moderately active and better than the *meta* isomer **12b** (18% inhibition at 50 μM) (Table 2). The two benzylphosphonic acids **12c** ($IC_{50} = 28.4 \pm 2.9 \mu M$) and **12d** ($IC_{50} = 18.9 \pm 1.1 \mu M$) showed improved activity compared to **12a**. The *N-p*-cyclohexylbenzyl group clearly contributes to the activity of **12a,c,d** since the unsubstituted amides **29a-c** are all significantly less active. The STAT3 inhibitory activity of **12d** indicated that the benzamide scaffold merited further attention.

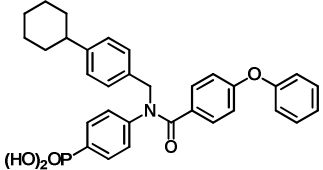
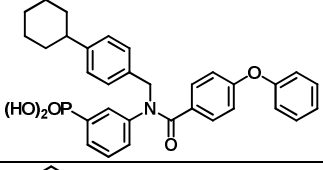
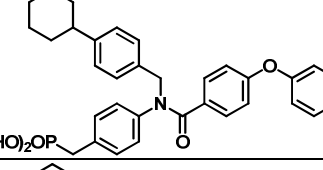
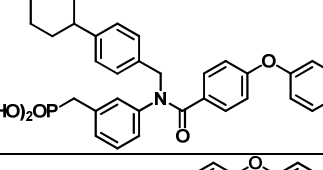
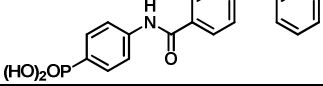
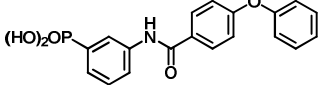
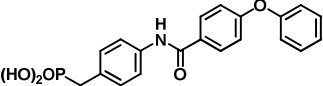
Since the phosphonates would likely require a prodrug protection strategy¹² to render them cell permeable, we next investigated salicylic acid containing *N*-benzamides **13**. The analog of **12d** with a simple unsubstituted *N*-benzyl substituent was inactive (Table 3, **13a**, 3% inhibition at 50 μ M). The 4-methoxybenzyl derivative **13b** was weakly active (IC_{50} 118.1 \pm 8.6 μ M) as was its 3,4-dimethoxy analog **13c**. Some improvement in activity was observed when the R substituent was a halogen (**13d**, IC_{50} 48 \pm 9.4 μ M and **13e**, IC_{50} 52 \pm 4.3 μ M). The presence of an alkyl group (R = *n*-heptyl and cyclohexyl, Table 3) resulted in further improvement (**13f**, IC_{50} 12.8 \pm 0.5 μ M and **13g**, IC_{50} 15 \pm 4.4 μ M respectively). This effect of the *para*-alkyl group of the *N*-benzylamide of **11f-h** also resulted in analogs with similar activities (Table 1). Replacement of the phenoxybenzoyl group of **13f** (IC_{50} 12.8 \pm 0.5 μ M) by benzoyl (**13h**, IC_{50} 32 \pm 4 μ M) and 3-methoxybenzoyl (**13i**, IC_{50} 33.3 \pm 1.6 μ M) resulted in a two-fold reduction in activity in both cases. Substitution of the phenyl group of **13h** by a pyridyl group as in **13j**, **13k** and **13l** resulted in significant reduction in activity. The carboxylic acid **33**, an isomer of **13g**, possessing the isomeric salicylic acid group, was prepared from 4-amino-2-hydroxybenzoic acid (Scheme S2, Supporting Information). This was essentially inactive in the FP assay (12% inhibition at 50 μ M and 24% at 200 μ M). At least in this case the 5-amino-2-hydroxybenzoic acid of **13g** is critical for activity.

Table 1: *In vitro* FP inhibitory activity, for disruption of the STAT3–pYLPQTV complex, of library 11

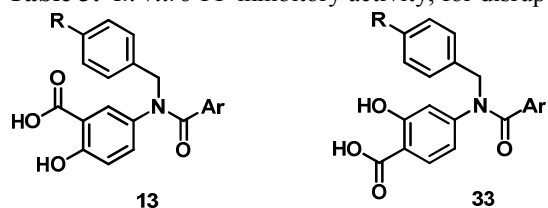
Compound	R	R ¹	Ar	IC ₅₀ (μM) ^a
11a	H	Bn		201.3 ± 1.5
11b	H	Bn		22.2 ± 9.1
11c	Cl	Bn		50 ± 3.8
11d	Cl	Bn		15 ± 1.2
11e	OCH ₃	Bn		22 ± 10
11f		Bn		23.3 ± 2
11g	<i>n</i> -C ₇ H ₁₃	Bn		19 ± 3.5
11h	<i>iso</i> -Butyl	Bn		17 ± 3.6
11i	H	Me		> 1000
11j	H	Me		57 ± 13
11k	Cl	Me		61 ± 6
11l		Me		45 ± 12
11m		Me		32 ± 12
11n	<i>n</i> -C ₇ H ₁₃	Me		22 ± 8
11o	<i>iso</i> -Butyl	Me		20 ± 7.1
11p	Cl	Me		43 ± 6
11q	OCH ₃	Me		50 ± 9.1
11r	<i>n</i> -C ₇ H ₁₃	Me		23 ± 0.3
11s	4-Piperidyl	Bn		>300
11t	3-(4-Pyridyl)	Bn		33.5 ± 1.8
11u	4-Morpholinyl	Bn		94.7 ± 0.32
11v	4-Piperidyl	Me		14.4 ± 0.6% inhibition at 50 μM
11w	3-(4-Pyridyl)	Me		35.3 ± 12.7

a: The IC₅₀ is defined as the concentration that gives an FP signal half that of the difference between the bound and free states of the STAT3–pYLPQTV complex (see supporting information).

Table 2: *In vitro* FP inhibitory activity, for disruption of the STAT3–pYLPQTV complex, of libraries **12** and **29**.

Compound	Structure	IC ₅₀ (μM) ^a
12a		42.0 ± 0.8
12b		17.9 ± 0.5% inhibition at 50 μM
12c		28.4 ± 2.9
12d		18.9 ± 1.1
29a		7.0 ± 2.9% inhibition at 50 μM
29b		9.0 ± 1.7% inhibition at 50 μM
29c		32.8 ± 6.3% inhibition at 50 μM

a: The IC₅₀ is defined as the concentration that gives an FP signal half that of the difference between the bound and free states of the STAT3–pYLPQTV complex (see supporting information).

Table 3: *In vitro* FP inhibitory activity, for disruption of the STAT3-pYLPQTV complex, of library 13.

Compound	R	Ar	IC ₅₀ (μM) ^a unless otherwise specified
13a	H		3% inhibition at 50 μM
13b	OMe		118.1 ± 8.6
13c	3,4-Di-OMe ^b		13 ± 8% inhibition at 50 μM
13d	Cl		48 ± 9.4
13e	Br		52 ± 4.3
13f	Heptyl		12.8 ± 0.5
13g	Cyclohexyl		15 ± 4.4
13h	Heptyl		32 ± 4
13i	Heptyl		33.3 ± 1.6
13j	Heptyl		22 ± 5% inhibition at 50 μM
13k	Heptyl		21 ± 3% inhibition at 50 μM
13l	Heptyl		31 ± 6% inhibition at 50 μM
33	Cyclohexyl		12 ± 0.2% inhibition at 50 μM

a: The IC₅₀ is defined as the concentration that gives an FP signal half that of the difference between the bound and free states of the STAT3-pYLPQTV complex (see supporting information). b: indicates 3,4-disubstitution of the phenyl group bearing the R substituent.

The phosphonic acid **12d**, and salicylic acids **13f** and **13g** were docked to the STAT3 SH2 using GLIDE, using methods described previously.²⁴ The low-energy docking poses are shown in Figure 3 position the acidic groups in the pTyr-705 binding site and are broadly similar. The superimposition of all three inhibitors **12d** (green), **13f** (yellow) and **13g** (blue) is shown in Figure 3a. The *meta*-phosphonic acid group of **12d** occupies the phenylphosphate binding pocket (Figure 3b). Indeed, the phosphorus atom is only 0.2 Å from the position of the STAT3 pTyr-705 residue X-ray coordinates (see Figure S1, supporting information). Hydrogen bonds are formed between the three phosphate oxygen atoms and with residues Lys-591, Arg-609, Glu-612 and Ser-611 (Figure 3c). Charged interactions are evident between the phosphonate and the Lys-591 and Arg-609 residues. The phenoxybenzoyl group is positioned with the terminal phenyl group occupying the pY+1 hydrophobic pocket. The *p*-cyclohexylbenzyl group places the cyclohexyl group deep within the hydrophobic pY-X pocket.³⁴

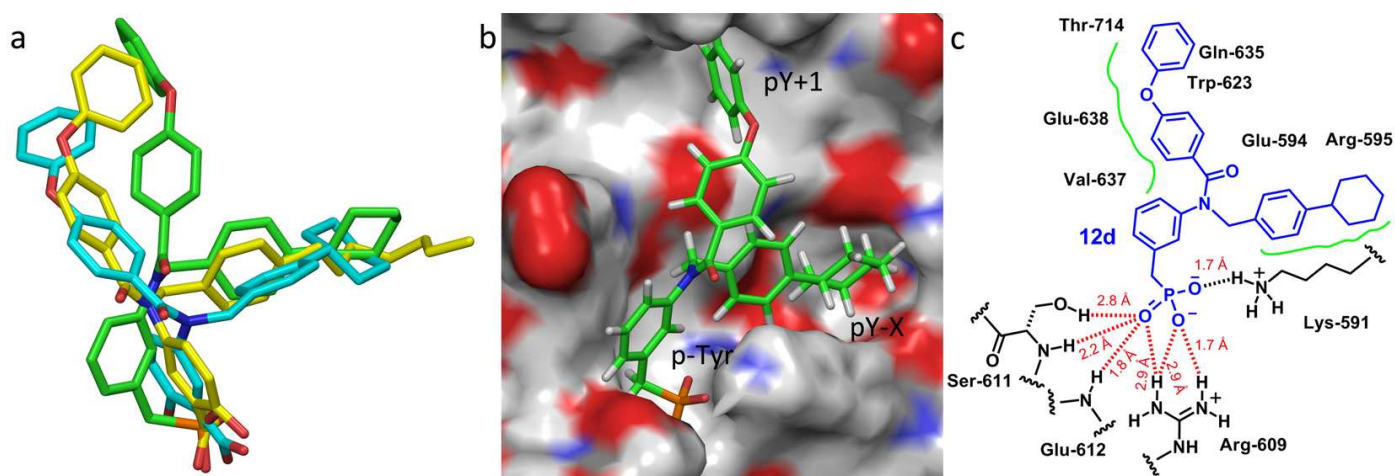


Figure 3. Docking of phosphonic acid **12d** and salicylic acids **13f** and **13g** to the STAT3 SH2 domain. *a*: overlay of the docked poses of phosphonate **12d** (carbon atoms shown green) and salicylic acids **13f** (carbon atoms shown yellow) and **13g** (carbon atoms shown blue) with hydrogen atoms omitted. *b*: surface rendering of **12d** docked to the STAT3 p-Tyr binding site (carbon and hydrogen atoms shown gray; oxygen atoms shown red and nitrogen atoms shown blue). *c*: Schematic binding mode of **12d** to the STAT3 SH2 domain showing the hydrogen bonds (red) and hydrophobic interactions (green).

The salicylic acids **13f** and **13g** dock with their hydroxycarboxylic acid groups deep within the p-Tyr binding site. The docking pose of **13g**, discussed in detail elsewhere,³⁵ positions its *p*-cyclohexylbenzyl group in the pY-X pocket and the phenoxyphenyl group in a region close to the pY+1 pocket. A similar pose is also obtained for salicylic acid **13f** (shown in yellow in Figure 3a) with the *p*-heptylbenzyl group occupying the pY-

X pocket. The terminal phenyl group of the phenoxybenzoyl group is located in the pY+1 pocket (see Figure S2a, supporting information). Overall the docking shows that all three molecules are able to adopt reasonable conformations that results in polar interactions of the acid group with the p-Tyr binding pocket and hydrophobic interaction of each of the sides chains in both the pY-X pocket and the area close to or in pY+1 pocket.

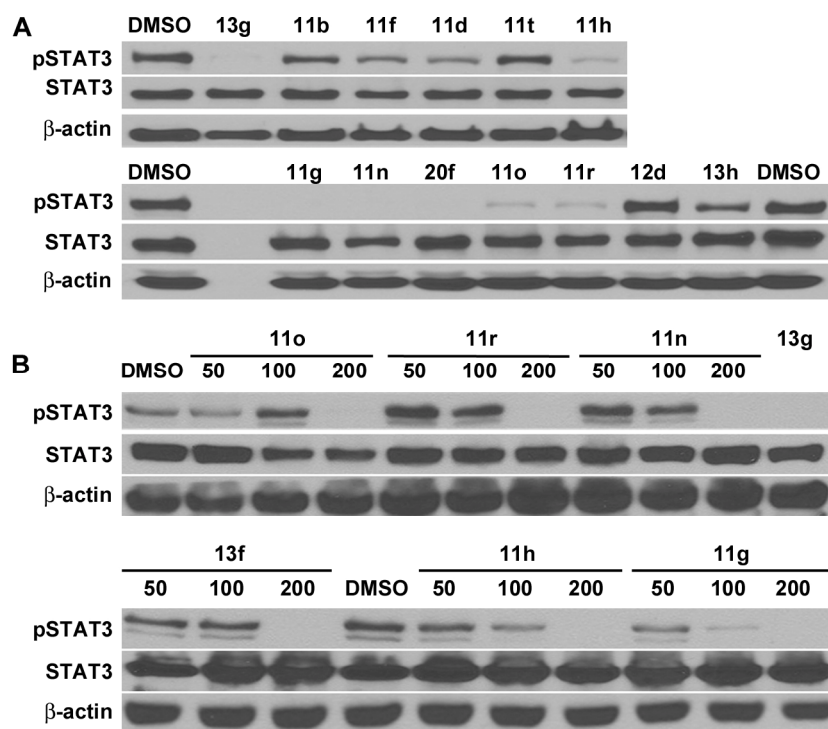


Figure 4. Effects of selected compounds upon pSTAT3 levels in MDA-MB-468 human breast cancer cell lines after 4 h treatment by immunoblotting. A: treatment at single dose of 200 μ M for all compounds. B: Dose response for selected compounds at 50, 100 and 200 μ M.

A selection of the most potent compounds in the FP assay from the libraries **11**, **12** and **13** were assessed in a cellular assay. Their potency derives from their ability to displace fluorescein-GpYLPQTV suggesting that they bind at the phosphotyrosine-705 binding site in the SH2 domain of STAT3. STAT3 is known to be phosphorylated on Y705 by the EGF receptor (EGFR) tyrosine kinase. This phosphorylation of Y705 is preceded by recruitment of STAT3 to EGFR by binding of the STAT3-SH2 domain to pY1068 or pY1086 of EGFR.³⁶ A compound binding to the SH2 domain of STAT3 is therefore expected to block the binding of STAT to EGFR and subsequent phosphorylation of Y705 of STAT3. Human breast cancer MDA-MB-468 cells

were treated with the compounds (200 μM) and the levels of pSTAT3 assessed by immunoblotting after 4 hours (Figure 4A). Most of the compounds reduced the amount of pSTAT3. It was not surprising that the phosphonic acid **12d** did not affect the pSTAT3 levels, since phosphonic acids are not usually cell permeable. Five of the best compounds, **11o**, **11r**, **11n**, **11h**, and **13f** were then tested at 50, 100 and 200 μM (Figure 4B) and the results as shown in Figure 4B indicate that inhibition of pSTAT3 was dose dependent. At 100 μM **11o** appears to increase pSTAT3 and decrease total STAT3 and therefore at this concentration may have activated STAT3. Nevertheless at 200 μM it is clear that for all compounds shown in Figure 4B that STAT3 is significantly deactivated. These results are consistent with the ability of the compounds to block the binding of the fluorescent labeled peptide to the STAT3 SH2 domain. One compound, the benzamide **13g**, was selected for further biological characterization. Its ability to inhibit STAT3 dimerization *in vitro* and in intact cells and to suppress malignant transformation in human cancer cells that depend on STAT3 is reported by us in detail elsewhere.³⁵

In conclusion, we have shown that the phosphotyrosine mimicking 5-amino-2-hydroxybenzoic acid can be incorporated into analogs of **1** and provides significantly active STAT3 dimerization inhibitors. We have also developed a series of *N*-benzylbenzamides **13** by removing the reactive sulfonyloxymethyl moiety of the linking group of **1**, as STAT3 dimerization inhibitors with improved potency. Importantly, the equivalent potencies of **13g** and **12d** further validates 5-amino-2-hydroxybenzoic acid as a phosphotyrosine mimic.

Acknowledgments

We thank the Moffitt Chemical Biology Core for their outstanding technical assistance and maintenance of the NMR, mass spectrometry and HPLC instruments. This work was partially supported by NCI grant CA140681 (SMS and NJL).

Supporting Information: Experimental details of the compound synthesis and characterization, the FP assay and molecular modeling. Figures S1 and S2 and Schemes S1 and S2.

References

1. J. E. Darnell, Jr., *Science*, 1997, **277**, 1630-1635.
2. J. E. Darnell, *Nat. Med.*, 2005, **11**, 595-596.
3. H. Yu and R. Jove, *Nat. Rev. Cancer*, 2004, **4**, 97-105.
4. P. Yue and J. Turkson, *Expert Opin. Inv. Drug*, 2009, **18**, 45-56.
5. D. Masciocchi, A. Gelain, S. Villa, F. Meneghetti and D. Barlocco, *Future Med. Chem.*, 2011, **3**, 567-597.
6. A. K. Mankan and F. R. Greten, *Expert Opin. Inv. Drug*, 2011, **20**, 1263-1275.
7. A. Lavecchia, C. Di Giovanni and E. Novellino, *Curr. Med. Chem.*, 2011, **18**, 2359-2375.
8. B. D. Page, D. P. Ball and P. T. Gunning, *Expert Opin. Ther. Pat.*, 2011, **21**, 65-83.
9. J. L. Yap, J. Chauhan, K.-Y. Jung, L. Chen, E. V. Prochownik and S. Fletcher, *MedChemComm*, 2012, **3**, 541-551.
10. J. Turkson, D. Ryan, J. S. Kim, Y. Zhang, Z. Chen, E. Haura, A. Laudano, S. Sebti, A. D. Hamilton and R. Jove, *J. Biol. Chem.*, 2001, **276**, 45443-45455.
11. D. R. Coleman, Z. Ren, P. K. Mandal, A. G. Cameron, G. A. Dyer, S. Muranjan, M. Campbell, X. Chen and J. S. McMurray, *J. Med. Chem.*, 2005, **48**, 6661-6670.
12. P. K. Mandal, F. Gao, Z. Lu, Z. Ren, R. Ramesh, J. S. Birtwistle, K. K. Kaluarachchi, X. Chen, R. C. Bast, W. S. Liao and J. S. McMurray, *J. Med. Chem.*, 2011, **54**, 3549-3563.
13. P. K. Mandal, D. Limbrick, D. R. Coleman, G. A. Dyer, Z. Ren, J. S. Birtwistle, C. Xiong, X. Chen, J. M. Briggs and J. S. McMurray, *J. Med. Chem.*, 2009, **52**, 2429-2442.
14. P. K. Mandal, Z. Ren, X. Chen, C. Xiong and J. S. McMurray, *J. Med. Chem.*, 2009, **52**, 6126-6141.
15. J. Chen, L. Bai, D. Bernard, Z. Nikolovska-Coleska, C. Gomez, J. Zhang, H. Yi and S. Wang, *ACS Med. Chem. Lett.*, 2010, **1**, 85-89.
16. M. Zhao, B. Jiang and F. H. Gao, *Curr. Med. Chem.*, 2011, **18**, 4012-4018.
17. W. Hao, Y. Hu, C. Niu, X. Huang, C.-P. B. Chang, J. Gibbons and J. Xu, *Bioorg. Med. Chem. Lett.*, 2008, **18**, 4988-4992.
18. K. Matsuno, Y. Masuda, Y. Uehara, H. Sato, A. Muroya, O. Takahashi, T. Yokotagawa, T. Furuya, T. Okawara, M. Otsuka, N. Ogo, T. Ashizawa, C. Oshita, S. Tai, H. Ishii, Y. Akiyama and A. Asai, *ACS Med. Chem. Lett.*, 2010, **1**, 371-375.
19. J. Schust, B. Sperl, A. Hollis, T. U. Mayer and T. Berg, *Chem. Biol.*, 2006, **13**, 1235-1242.
20. H. Song, R. X. Wang, S. M. Wang and J. Lin, *P. Natl. Acad. Sci. USA*, 2005, **102**, 4700-4705.
21. V. M. Shahani, P. Yue, S. Haftchenary, W. Zhao, J. L. Lukkarila, X. Zhang, D. Ball, C. Nona, P. T. Gunning and J. Turkson, *ACS Med. Chem. Lett.*, 2011, **2**, 79-84.
22. K. A. Z. Siddiquee, P. T. Gunning, M. Glenn, W. P. Katt, S. Zhang, C. Schroeck, S. M. Sebti, R. Jove, A. D. Hamilton and J. Turkson, *ACS Chem. Biol.*, 2007, **2**, 787-798.
23. H. Li, A. Liu, Z. Zhao, Y. Xu, J. Lin, D. Jou and C. Li, *J. Med. Chem.*, 2011, **54**, 5592-5596.

24. K. Siddiquee, S. Zhang, W. C. Guida, M. A. Blaskovich, B. Greddy, H. R. Lawrence, M. L. R. Yip, R. Jove, M. M. McLaughlin, N. J. Lawrence, S. M. Sebti and J. Turkson, *P. Natl. Acad. Sci. USA*, 2007, **104**, 7391-7396.
25. S. Becker, B. Groner and C. W. Muller, *Nature*, 1998, **394**, 145-151.
26. L. Lin, R. Amin, G. I. Gallicano, E. Glasgow, W. Jogunoori, J. M. Jessup, M. Zasloff, J. L. Marshall, K. Shetty, L. Johnson, L. Mishra and A. R. He, *Oncogene*, 2009, **28**, 961-972.
27. S. Fletcher, B. D. G. Page, X. Zhang, P. Yue, Z. H. Li, S. Sharmeen, J. Singh, W. Zhao, A. D. Schimmer, S. Trudel, J. Turkson and P. T. Gunning, *ChemMedChem*, 2011, **6**, 1459-1470.
28. S. Fletcher, J. Singh, X. Zhang, P. Yue, B. D. G. Page, S. Sharmeen, V. M. Shahani, W. Zhao, A. D. Schimmer, J. Turkson and P. T. Gunning, *ChemBioChem*, 2009, **10**, 1959-1964.
29. X. Zhang, P. Yue, B. D. G. Page, T. Li, W. Zhao, A. T. Namanja, D. Paladino, J. Zhao, Y. Chen, P. T. Gunning and J. Turkson, *P. Natl. Acad. Sci. USA*, 2012, **109**, 9623-9628.
30. I. Azumaya, T. Okamoto, F. Imabeppu and H. Takayanagi, *Tetrahedron*, 2003, **59**, 2325-2331.
31. T. R. Burke, Jr., M. S. Smyth, A. Otaka, M. Nomizu, P. P. Roller, G. Wolf, R. Case and S. E. Shoelson, *Biochemistry*, 1994, **33**, 6490-6494.
32. J. Schust and T. Berg, *Anal. Biochem.*, 2004, **330**, 114-118.
33. Z. Ren, L. A. Cabell, T. S. Schaefer and J. S. McMurray, *Bioorg. Med. Chem. Lett.*, 2003, **13**, 633-636.
34. I.-H. Park and C. Li, *J. Mol. Recognit.*, 2011, **24**, 254-265.
35. X. Zhang, Y. Sun, R. Pireddu, H. Yang, M. K. Urlam, H. R. Lawrence, W. C. Guida, N. J. Lawrence and S. M. Sebti, *Cancer Res.*, Published OnlineFirst January 15, 2013, **73**, doi:10.1158/0008-5472.CAN-1112-3175
36. H. Shao, H. Y. Cheng, R. G. Cook and D. J. Tweardy, *Cancer Res.*, 2003, **63**, 3923-3930.